POSITION CONTROL OF ELECTRO-HYDRAULIC SERVO SYSTEM WITH FRICTION COMPENSATION

Michael Enyan[1*], Luis Miguel Ruiz Páez[1]

[1]*School of Mechanical Engineering, Jiangsu University, Zhenjiang 212013, P. R China.*

*Corresponding Author

ABSTRACT

This work presents a model-based friction compensation technique and an integral adaptive backstepping controller to improve the position control of the electrohydraulic servo system. The controller design uses a continuous approximation of the LuGre friction model and the Lyapunov theory of nonlinear systems. The friction compensation enhances system performance, and comparison tests are conducted on a hydraulic servo test bench to validate the control strategy's tracking performance under various conditions.
KEYWORDS: *Electrohydraulic servo systems; Position control; Integral adaptive backstepping controller; LuGre dynamic friction model; Lyapunov theory; Friction compensation.*

1. INTRODUCTION

Electrohydraulic servo systems (EHSS) are widely utilized in a variety of industrial applications and cutting-edge automation systems due to their outstanding characteristics, such as excellent positioning capabilities, a high-power ratio, rapid and effortless reaction, rigidity, and the capacity to create enormous amounts of force [1]. It has been used in a variety of mechanizations and has had a substantial impact on modern position control devices such as hydraulic robot manipulators [2,3], hydraulic presses [4], load simulators [2,5–7], vehicle active suspension systems [8–11], and aircraft actuators [6]. However, for precise positioning in these applications, a reliable electro-hydraulic actuator is required and also high-precision servo system must have low-speed stability as well as great tracking accuracy. As a result, the design of an appropriate extremely robust controller capable of reflecting these properties is critical. The EHSS's extremely nonlinear dynamic features [12,13], parameter fluctuations, modeling errors, and external disturbances are also significant barriers to obtaining high-accuracy position tracking performance. As a result, the EHSS's position-tracking problem has gained significant focus in the past few years and several efforts have been made to explore and resolve these issues [14–23].

Nevertheless, friction is the most intricate and difficult to address of the nonlinear elements that affect the performance of hydraulic systems. Because it is incredibly difficult to comprehend the mechanical contact phenomenon, obtaining precise friction

information to increase tracking performance is impossible [24–28].

Scholars have developed several compensating approaches to increase the effectiveness of the nonlinear servo control system to counteract the impact of friction disturbance on the control system's performance. According to [29], there are primarily two friction compensation strategies. The first approach is to develop a friction-based compensating controller. An alternate approach is the intelligent control technique that may be used to dampen the friction interruption by treating it as an external interference. According to [30], the most common types of friction models are dynamic friction models and static friction models. Armstrong's model, Coulomb's model, Stribeck's model, and Karnopp's model are the most common static friction models [31–34]. As a result of its simplistic structure and easily recognizable characteristics, the static friction model is often used for friction compensation, however, this approach only yields marginal gains in system performance since it fails to adequately capture the friction phenomena. Dynamic friction models have therefore also been studied by several researchers and these models mostly include the Dahl model, Elastoplastic model, LuGre model, and Leuven model [35–38].

Among the compensation approaches, the LuGre model [39] proposed by de Wit et al. is one of the most often used and effective approaches. Because the LuGre model represents the standard characteristics of the surfaces in direct contact in a

microscopic perspective and implements a nonlinear first-order differential equation to describe it, it can describe the principal frictional characteristics using a much simpler equation. However, any model can only be an approximation to real friction, and it is almost impossible to build a completely accurate model for friction. Several scholars have developed various control schemes using the LuGre friction model and achieved good engineering results [40–43].

In this paper, a nonlinear robust integral adaptive backstepping controller with friction compensation (w\FC) is designed for the position control of the electrohydraulic servo system. Two observers are built based on the LuGre model to describe the various nonlinear characteristics of the unmeasurable state and an integral adaptive backstepping controller is designed to achieve the friction compensation. As a result, the system's nonlinear friction and external disturbance are reduced, and position tracking is improved.

2. THE LUGRE FRICTION MODEL

According to [39], the LuGre dynamic friction model, the average deformation behavior based on the bristle is:

$$\frac{dz}{dt} = \dot{x} - \frac{|\dot{x}|}{g(\dot{x})}z \qquad (1)$$

where z, $g(\bullet)$ respectively represent the average deformation of the bristle and the friction model describing the static behavior of friction. The bristle's mean deformation z, is expressed as

$$z_{ss} = g(\dot{x})sign(\dot{x}) \qquad (2)$$

The friction force described by the LuGre model is

$$f_m = \sigma_0 z + \sigma_1 \frac{dz}{dt} + \sigma_2 \dot{x} \qquad (3)$$

where σ_0, σ_1 and σ_2 respectively represent the system bristle stiffness, damping, and viscous damping coefficient. And $g(\bullet)$ is the function that characterizes the static friction behavior, The exponential model is often used, i.e

$$g(\dot{x}) = \alpha_0 + \alpha_1 e^{-(\dot{x}/\dot{x}_s)^\lambda} \qquad (4)$$

In the formula, $\sigma_0 \alpha_0$, $\sigma_0(\alpha_0 + \alpha_1)$ respectively characterizes the macroscopic Coulomb friction f_C and static friction f_s, i.e

$$\sigma_0 g(\dot{x}) = f_c + (f_s - f_c)e^{-(\dot{x}/\dot{x}_s)^\lambda} \qquad (5)$$

3. CONTROL STRATEGY FOR FRICTION COMPENSATION BASED ON THE LUGRE MODEL
3.1 Design Model and Issues to be Addressed
Based on the EHSS model utilizing force balance equation, The hydraulic actuator's pressures, and the servo valve's flow equation as presented in [44] combined with the LuGre friction model from equation (3), define the state variables $x = [x_1, x_2, x_3]^T =$

$[y, \dot{y}, A_1P_1 - A_2P_2]^T$. Then, the nonlinear model of the EHSS can be written as:

$$\dot{z} = x_2 - \frac{|x_2|}{g(x_2)}z$$
$$\dot{x}_1 = x_2$$
$$m\dot{x}_2 = x_3 - \sigma_0 z + \sigma_1 \frac{|x_2|}{g(x_2)}z + (\sigma_1 + \sigma_2)$$
$$+ x_2 - d_n - \tilde{d}(x_1, x_2, t)$$
$$\dot{x}_3 = \left(\frac{A_1}{V_1}R_1 + \frac{A_2}{V_2}R_2\right)g\beta_e u$$
$$- \left(\frac{A_1^2}{V_1^2} + \frac{A_2^2}{V_2^2}\right)\beta_e x_2$$
$$- \left(\frac{A_1}{V_1} + \frac{A_2}{V_2}\right)\beta_e C_t P_L \qquad (6)$$

where, m, y, P_L, β_e, C_t are respectively system load mass, output displacement, the hydraulic cylinder's pressure difference, hydraulic oil elastic modulus, and actuator leakage coefficient, A_1, A_2 are the hydraulic cylinder's effective piston areas; V_1 and V_2 are the volumes of the cavities of the hydraulic cylinder; R_1, R_2 are defined as described above; g is the servo valve gain; d_n, is the concentration of unmodeled dynamics and external interference. Nominal value; $\tilde{d}(x_1, x_2, t) = f(x_1, x_2, t) - d_n$.

The following nonlinear function is defined

$$g_3(x) = \left(\frac{A_1}{V_1}R_1 + \frac{A_2}{V_2}R_2\right)g\beta_e > 0, \forall x$$
$$f_3(x) = \left(\frac{A_1^2}{V_1^2} + \frac{A_2^2}{V_2^2}\right)\beta_e x_2$$
$$+ \left(\frac{A_1}{V_1} + \frac{A_2}{V_2}\right)\beta_e C_t P_L \qquad (7)$$

The system unknown parameters are defined as $[\theta_1, \theta_1, \theta_1, \theta_1]^T = [\sigma_0, \sigma_1, \sigma_1 + \sigma_2, d_n]^T$ then equation (6) can be transformed into:

$$\begin{cases} \dot{z} = x_2 - \frac{|x_2|}{g(x_2)}z \\ \dot{x}_1 = x_2 \\ m\dot{x}_2 = x_3 - \theta_1 z + \theta_2 \frac{|x_2|}{g(x_2)}z - \theta_3 x_2 - \theta_4 - \tilde{d}(\\ \dot{x}_3 = g_3(x)u - f_3(x) \end{cases} \qquad (8)$$

Control goal: the design objective of the system controller is to design a control input u ensuring its boundedness for the given system reference signal $y_d(t) = x_{1d}(t)$, so that the system output $y = x_1$ can track the system reference signal as much as possible. The reference signal has the following assumptions: system reference command signal x_{1d} is third-order continuous, and the

expected system position command, velocity command, and acceleration command are bounded.

3.2 Design of integral adaptive backstepping controller

Because the system equations have mismatched parameter uncertainties and existing nonlinear friction, the backstepping design method is used. We design an integral adaptive backstepping controller based on Lyapunov stability theory to accomplish system stability and adaptive ability by making the system output approach the target trajectory with high approximation.

Step 1: From the system equation (8), define the error variables for the first two equations of (8) as

$$e_1 = x_1 - x_{1d}$$
$$e_2 = \dot{e}_1 + k_1 e_1 = x_2 - x_{2eq}, x_{2eq} \quad (9)$$
$$\stackrel{def}{=} \dot{x}_{1d} - k_1 e_1$$

where $e_1 = x_1 - x_{1d}$ is the system tracking error, and $k_1 > 0$ is positive feedback gain.

In the following controller design, the main design goal is to make e_2 approach 0. It can be seen from Equation (9).

$$m\dot{e}_2 = m\dot{x}_2 - m\dot{x}_{2eq}$$
$$= \theta_1 z + \theta_2 \frac{|x_2|}{g(x_2)} z \quad (10)$$
$$- \theta_3 x_2 - \theta_4 - \tilde{d} - m\dot{x}_{2eq}$$

In the controller design of this step, the observer structure is used to estimate the different properties of the state z, and the mapping function is used to ensure that the observer estimation is controlled to ensure that the observer is stable.

$$\hat{z}_1 = \mathrm{Pr}\,oj_{\hat{z}_1}(l_1), \qquad z_{min} \le z_1(0) \le z_{max}$$
$$\hat{z}_2 = \mathrm{Pr}\,oj_{\hat{z}_2}(l_2), \qquad z_{min} \le z_2(0) \le z_{max} \quad (11)$$

where l_1 and l_2 are the regulating functions of z_1 and z_2 observer respectively. For the different estimates of state z_1 and z_2, their upper and lower bounds are given respectively as $z_{1max} = z_{2max} = z_{max} = \alpha_0 + \alpha_1$, $z_{1min} = z_{2min} = z_{min} = -(\alpha_0 + \alpha_1)$ respectively. In Equation (11), the mapping function is defined as

$$\mathrm{Pr}\,oj_{\hat{\gamma}}(\bullet) = \begin{cases} 0, & \hat{\zeta} = \gamma_{max} \\ 0, & \hat{\zeta} = \gamma_{max} \\ \bullet, & otherwise \end{cases} \quad (12)$$

where γ can be an unknown parameter θ or system state z. For the unknown parameter θ, the following parameter adaptive law is defined;

$$\dot{\hat{\theta}} = \mathrm{Pr}\,oj_{\hat{\theta}}(\Gamma \tau), \qquad \theta_{min} \le \hat{\theta}(0) \le \theta_{max} \quad (13)$$

where $\dot{\hat{\theta}}$ represents the estimation of the unknown parameter θ of the system, and $\tilde{\theta} = \hat{\theta} - \theta$ is the error of parameter estimation; $\Gamma > 0$ is the positive definite diagonal matrix, and represents the adaptive gain; τ is the parametric adaptive function.

Based on the above-controlled parameter and state estimation, there is the following lemma:

Lemma 1; For any adaptive function τ, the observer adjustment functions l_1 and l_2 discontinuous mapping expression equation (12) has the following properties;

$$\theta_{min} \le \hat{\theta} \le \theta_{max} \quad (14)$$
$$z_{min} \le \hat{z}_1 \le z_{max} \quad (15)$$
$$z_{min} \le \hat{z}_2 \le z_{max} \quad (16)$$
$$\tilde{\theta}^T \left[\Gamma^{-1}\dot{\hat{\theta}} - \tau \right] \le 0, \forall \tau \quad (17)$$
$$\tilde{z}_1 \{\dot{\hat{z}}_1 - l_1\} \le 0 \quad (18)$$
$$\tilde{z}_1 \{\dot{\hat{z}}_1 - l_1\} \le 0 \quad (19)$$

In the formula, $\tilde{z}_1 \underline{def} \hat{z}_1 - z$, $\tilde{z}_2 \underline{def} \hat{z}_2 - z$ respectively represent the deviation of different state estimates, and have the following dynamic;

$$\frac{d\tilde{z}_1}{dt} = \hat{z}_1 - \dot{z} = \mathrm{Pr}\,oj_{\hat{z}_1}(l_1)$$
$$- \left(x_2 - \frac{|x_2|}{g(x_2)} z \right) \quad (20)$$
$$\frac{d\tilde{z}_2}{dt} = \hat{z}_2 - \dot{z} = \mathrm{Pr}\,oj_{\hat{z}_2}(l_2)$$
$$- \left(x_2 - \frac{|x_2|}{g(x_2)} z \right) \quad (21)$$

In other to make e_2 converge to zero or small and have a guaranteed transient response, we treat x_3 as virtual control input and construct a control function for it. The control function $\alpha_2(x_1, x_2, \hat{\theta}, \hat{z}_1, \hat{z}_2, t)$ for the dynamic equation (10) has the following structural form:

$$\alpha_2(x_1, x_{2,}\hat{\theta}, t) = \alpha_{2a} + \alpha_{2s}$$
$$\alpha_{2a} = \hat{\theta}_1 \hat{z}_1 - \hat{\theta}_2 \frac{|x_2|}{g(x_2)} \hat{z}_2 + \hat{\theta}_3 x_2 + \hat{\theta}_4 \quad (22)$$
$$+ m\dot{x}_{2eq}$$
$$\alpha_{2s} = \alpha_{2s1} + \alpha_{2s2}$$
$$\alpha_{2s1} = -k_{2s1} e_2$$

where, $k_{2s1} > 0$ is a controller design parameter. The feedback gain k_1, and k_{2s1} is large enough to make the matrix Λ_2 below a positive definite matrix:

$$\Lambda_2 = \begin{pmatrix} k_1{}^3 & -\dfrac{1}{2}k_1{}^3 \\ -\dfrac{1}{2}k_1{}^3 & k_{2s1} \end{pmatrix} \qquad (23)$$

The error between the control function α_2 and the virtual control input x_3 is defined as: $e_3 = x_3 - \alpha_2$ and substitute equation (22) into Equation (10) then we obtain

$$\begin{aligned} m\dot{e}_2 = e_3 &- k_{2s1}e_2 + \alpha_{2s2} - \varphi_2{}^T\tilde{\theta} \\ &+ \theta_1\tilde{z}_1 - \theta_2\frac{|x_2|}{g(x_2)}\tilde{z}_2 - \tilde{d} \end{aligned} \qquad (24)$$

Where:

$$\varphi_2{}^T \underline{def} \left[-\hat{z}_1, \frac{|x_2|}{g(x_2)}\hat{z}_2, -x_2, -1\right] \qquad (25)$$

According to Equation (24) α_{2s2} is designed to satisfy the following stabilization conditions;

$$e_2\left\{\alpha_{2s2} - \varphi_2{}^T\tilde{\theta} - \theta_1\tilde{z}_1 - \theta_2\frac{|x_2|}{g(x_2)}\tilde{z}_2 \right. \\ \left. - \tilde{d}\right\} \le \varepsilon_2 \qquad (26)$$

$$e_2\alpha_{2s2} \le 0 \qquad (27)$$

Where, ε_2 is the controller design parameter that can be arbitrarily small and positive. As can be seen from equation (26) the designed α_{2s2} is a robust controller.

Define the following Lyapunov function:

$$V_2 = \frac{1}{2}me_2{}^2 + \frac{1}{2}k_1{}^2e_1{}^2 \qquad (28)$$

And its time differential is

$$\begin{aligned} \dot{V}_2 &= m\dot{e}_2e_2 + k_1{}^2e_1\dot{e}_1 \\ &= e_2e_3 - k_1{}^3e_1{}^2 + k_1{}^2e_1e_2 - k_{2s1}e_2{}^2 \\ &\quad + e_2\{\alpha_{2s2} - \varphi_2{}^T\tilde{\theta} - \theta_1\tilde{z}_1 \\ &\quad - \theta_2\frac{|x_2|}{g(x_2)}\tilde{z}_2 - \tilde{d}\} \end{aligned} \qquad (29)$$

Step 2: In the first step, from equation (29), it can be seen that if $e_3 = 0$, the condition equation (26) and equation (27) will achieve position tracking. The purpose of this step 2 is to design the actual control law u in such a way that x_3 tracks the virtual control

function α_2 as well as guarenteering transient perfomance. According to the third equation of the system from equation (8), and the definition of e_3 we get:

$$\dot{e}_3 = g_3u - f_3 - \dot{\alpha}_2 \qquad (30)$$

where:

$$\begin{aligned} \dot{\alpha}_2 &= \dot{\alpha}_{2c} - \dot{\alpha}_{2u} \\ \dot{\alpha}_{2c} &= \frac{\partial\alpha_2}{\partial t} + \frac{\partial\alpha_2}{\partial x_1}x_2 + \frac{\partial\alpha_2}{\partial x_2}\hat{x}_2 + \frac{\partial\alpha_2}{\partial\hat{\theta}}\dot{\hat{\theta}} \\ &\quad + \frac{\partial\alpha_2}{\partial\hat{z}_1}\dot{\hat{z}} + \frac{\partial\alpha_2}{\partial\hat{z}_2}\dot{\hat{z}} \end{aligned} \qquad (31)$$

$$\dot{\alpha}_{2u} = \frac{\partial\alpha_2}{\partial x_2}\tilde{\hat{x}}_2$$

of which:

$$\begin{aligned} \hat{x}_2 \,\underline{def}\, &\frac{x_3 - \hat{\theta}_1\hat{z}_1\dfrac{|x_2|}{g(x_2)}\hat{z}_2 - \hat{\theta}_3x_2 - \hat{\theta}_4}{m} \\ \tilde{x}_2 \,\underline{def}\, &\frac{\varphi_2{}^T\tilde{\theta} - \theta_1\tilde{z}_1\dfrac{|x_2|}{g(x_2)}\tilde{z}_2 + \tilde{d}}{m} \end{aligned} \qquad (32)$$

Equation (31), $\dot{\alpha}_{2c}$ is the computable partial differential part $\dot{\alpha}_2$, so it can be used in the design of actual controller u; $\dot{\alpha}_{2u}$ is the non-computable part $\dot{\alpha}_2$, a robust controller will be designed to stabilize this uncertainty. Although α_2 has a discontinuous function x_2 of x_2 when calculating the partial derivative of $|x_2|$, its limit of the partial derivative of $x_2 = 0$ is bounded.

According to Formula (30) and Formula (31) and the inequality in Formula (7), the control input signal u can be designed with the structure:

$$\begin{aligned} u &= u_a + u_s \\ u_a &= \frac{1}{g_3}(f_3 + \alpha_{2c}) \\ u_s &= \frac{1}{g_3}(u_{s1} + u_{s2}) \\ u_{s1} &= -k_{3s1}z_3 \end{aligned} \qquad (33)$$

where, $k_{3s1} > 0$ is the controller design parameter. The design feedback gain k_1, k_{2s1}, k_{3s1} is large enough to make the matrix Λ as below a positive definite matrix:

$$\Lambda = \begin{pmatrix} k_1{}^3 & -\dfrac{1}{2}k_1{}^3 & 0 \\ -\dfrac{1}{2}k_1{}^3 & k_{2s1} & -\dfrac{1}{2} \\ 0 & -\dfrac{1}{2} & k_{3s1} \end{pmatrix} \qquad (34)$$

By substituting the control law equation (33) into equation (30) we obtain

$$\dot{e}_3 = -k_{3s1}e_1 + u_{s2} - \varphi_2{}^T\tilde{\theta} - \frac{1}{m}\frac{\partial\alpha_2}{\partial x_2}\theta_1\tilde{z}_1$$
$$+ \frac{1}{m}\frac{\partial\alpha_2}{\partial x_2}\theta_2\frac{|x_2|}{g(x_2)}\tilde{z}_2 \qquad (35)$$
$$+ \frac{1}{m}\frac{\partial\alpha_2}{\partial x_2}\tilde{d}$$

where:

$$\varphi_3{}^T \underline{def} - \frac{1}{m}\frac{\partial\alpha_2}{\partial x_2}\varphi_2{}^T \qquad (36)$$

According to equation (35) u_{s2} can be designed to meet the following stabilization condition:

$$e_3\left\{ u_{s2} - \varphi_3{}^T\tilde{\theta} - \frac{1}{m}\frac{\partial\alpha_2}{\partial x_2}\theta_1\tilde{z}_1 \right.$$
$$+ \frac{1}{m}\frac{\partial\alpha_2}{\partial x_2}\theta_2\frac{|x_2|}{g(x_2)}\tilde{z}_2 \qquad (37)$$
$$\left. + \frac{1}{m}\frac{\partial\alpha_2}{\partial x_2}\tilde{d} \right\} \le \varepsilon_3$$

$$e_3 u_{s2} \le 0 \qquad (38)$$

where, ε_3 is the controller design parameter that can be arbitrarily small and positive. According to formula (37), u_{s2} designed is a robust controller.

The controller (33) designed has the following properties:

All signals in the closed-loop controller are bounded, and the Lyapunov function is defined as follows:

$$V_3 = V_2 + \frac{1}{2}e_3^2 \qquad (39)$$

And the inequality below is satisfied

$$V_3 \le \exp(-\mu t)V_3(0) + \frac{\varepsilon}{\mu}[1 - \exp(-\mu t)] \qquad (40)$$

where $\mu = 2\lambda_{\min(\Lambda_3)}\min\left\{\frac{1}{k_1^2}, \frac{1}{m}, 1\right\}$, $\lambda_{min}(\Lambda_3)$ is the minimum eigenvalue of the positive definite matrix Λ_3; $\varepsilon = \varepsilon_2 + \varepsilon_3$.

If after a certain time t_0, there is only parametric uncertainty in the system, i.e $\tilde{d} = 0$, then the controller (33) can also obtain asymptotic tracking performance i.e. when $t \to \infty, e \to 0$, where e is defined as $e = [e_1, e_2, e_3]^T$. The properties demonstrate that the developed controller can ensure the specified transient performance and final asymptotic tracking accuracy of the output. When the specified time has elapsed, the tracking error can be reduced to a satisfactory level as proved by [45]

Table 1. EHSS system parameters

Parameter	Value	Parameter	Value
$A_1 = A_2$ (m2)	6.409×10-4	m (kg)	40
P_s (Pa)	7×106	C_t (m5·N·s-1)	7×10-12
(Pa)	7×108	B (N/(m/s))	7500
$V_1 = V_2$ (m3)	3×10-2	K_q (m2/s)	0.874
σ_0 (N/m)	1×104	f_c (N)	41
σ_1 (N.s/m)	1×102	Strikback velocity x_{2s} (m/s)	0.01
$\tilde{d}$	0	d_n (N)	0
ρ (kg/m-3)	870	σ_2 (N.s/m)	70

4. EXPERIMENTAL SETUP AND RESULTS

The experimental findings of the EHSS position control are reported here. The experimental test bent is depicted in Figure 1(a). The control system is based on a real-time operating system using xPC target real-time online rapid prototyping control technology shown in Figure 1(b). The written program is compiled and downloaded to an industrial real-time control computer, which incorporates an in-line PCI slot for faster installation. The system uses a displacement sensor to input real-time dynamic signals from the actuator, and a closed-loop control is formed to move according to the set motion trajectory and condition. The sensor signals are stored on the host computer for further processing and analysis. The experiment consists of three scenarios of sinusoidal signal at various amplitudes and frequencies with 30mm amplitude and system subjected to double load as external disturbance. The tracking performance and bounded steady-state error of controllers are compared. The system's position tracking

performance and bounded trajectory tracking error are also examined under different conditions.

To verify the proposed controller's performance, the PID controller tuned to its best performance, and the traditional backstepping controller was compared. Results are presented in Figure 2 to Figure 4. The control gains which provided the best performance in the PID controller was $K_p = 3.1$, $K_i = 0.1$, and

$K_p = 0.001$. and the BSC design parameters were $K_1 = 27500$, $K_2 = 185$, and $K_3 = 60$. Proposed controller's parameters: $\gamma_1 = 1 \times 10^{-5}$, $\gamma_2 = 1 \times 10^{-5}$ $k_1 = 39500$, $k_2 = k_{2s1} + k_{2s2} = 200$, $k_2 = k_{3s1} + k_{3s2} = 55$, $\theta_{min} = [0.6 \times 10^5, 0.6 \times 10^5 \times (1 \times 10^5)^{0.5}, 55, -50]^T$, $\theta_{max} = [1 \times 10^5, 1 \times 10^5 \times (1 \times 10^5)^{0.5}, 70, 50]^T$, $\Gamma = diag\{2 \times 10^8, 1 \times 10^4, 195, 50\}$, $\theta(0) = [0.6 \times 10^5, 0.6 \times 10^5 \times (1 \times 10^5)^{0.5}, 55, 0]^T$
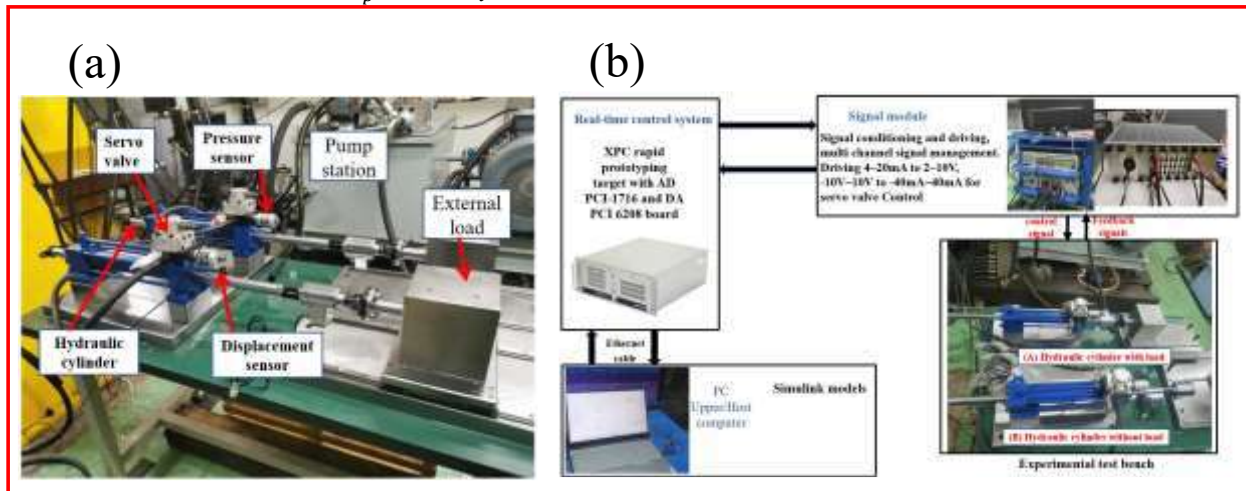
Figure 1. Experimental setup (a) Schematic of the experimental test bench. (b) Experimental control system.

The study also employed the mean square error (MSE), root mean square error ($RMSE$), maximum absolute tracking error ($RMSE$), and standard deviation (σ) of the tracking error values to evaluate controllers' performance. Results are presented in

Table **2**.

Table 2. Performance index

Controller	Error	MSE	RMSE	M_e	σ
30 mm and 0.25 Hz					
PID	0.55	0.0667	0.2583	0.3543	0.2581
BSC	0.385	0.0164	0.1281	0.2382	0.1261
w\FC	0.29	0.0032	0.0567	0.1303	0.0522
30 mm and 0.5 Hz					
PID	0.7	0.1877	0.4332	0.6158	0.4326
BSC	0.45	0.0482	0.2195	0.3296	0.2180
w\FC	0.3	0.0094	0.0968	0.2246	0.0832
50 mm and 0.25 Hz					
PID	0.459	0.1152	0.3393	0.4812	0.3393
BSC	0.199	0.0199	0.1410	0.1931	0.1405
w\FC	0.182	0.0116	0.1075	0.1864	0.0613
50 mm and 0.5 Hz					
PID	0.98	0.3768	0.6138	0.9111	0.6146
BSC	0.50	0.0824	0.2870	0.4042	0.2862
w\FC	0.37	0.032	0.1779	0.2626	0.1314
30 mm and 0.5 Hz with external disturbance					
PID	0.85	0.3043	0.5517	0.8854	0.5543
BSC	0.45	0.060	0.2468	0.4634	0.2526

| BSCF | 0.35 | 0.011 | 0.1054 | 0.3408 | 0.1186 |
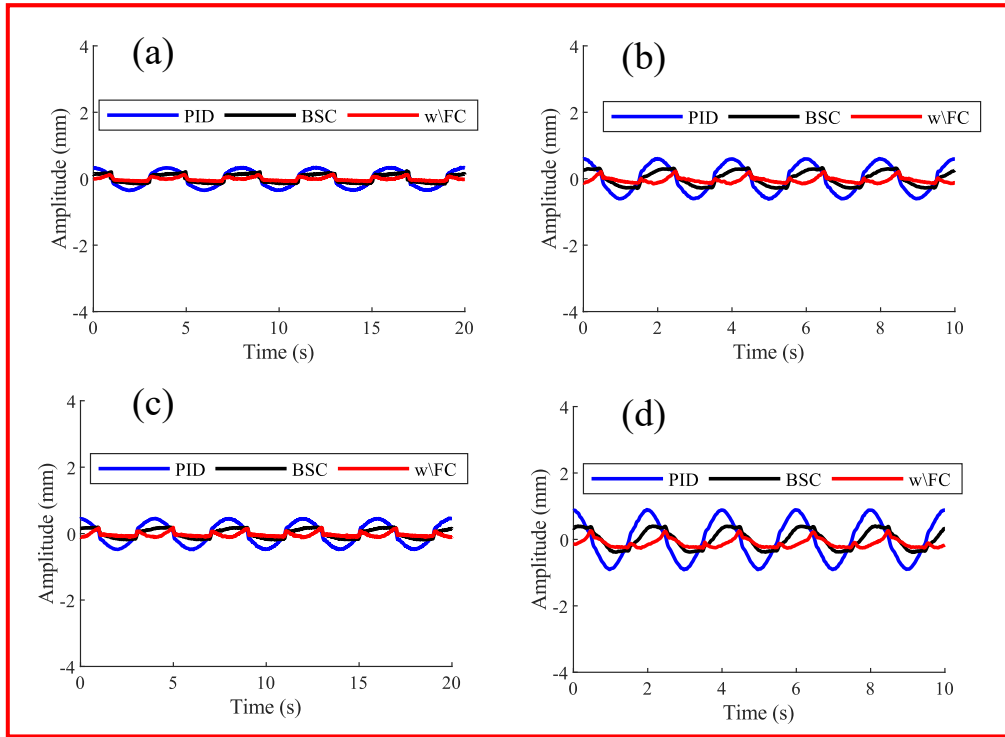
Figure 2. Tracking errors (a) 30 mm and 0.25 Hz (b) 30 mm and 0.5 Hz (c) 50 mm and 0.25 Hz (d) 50 mm and 0.5 Hz.
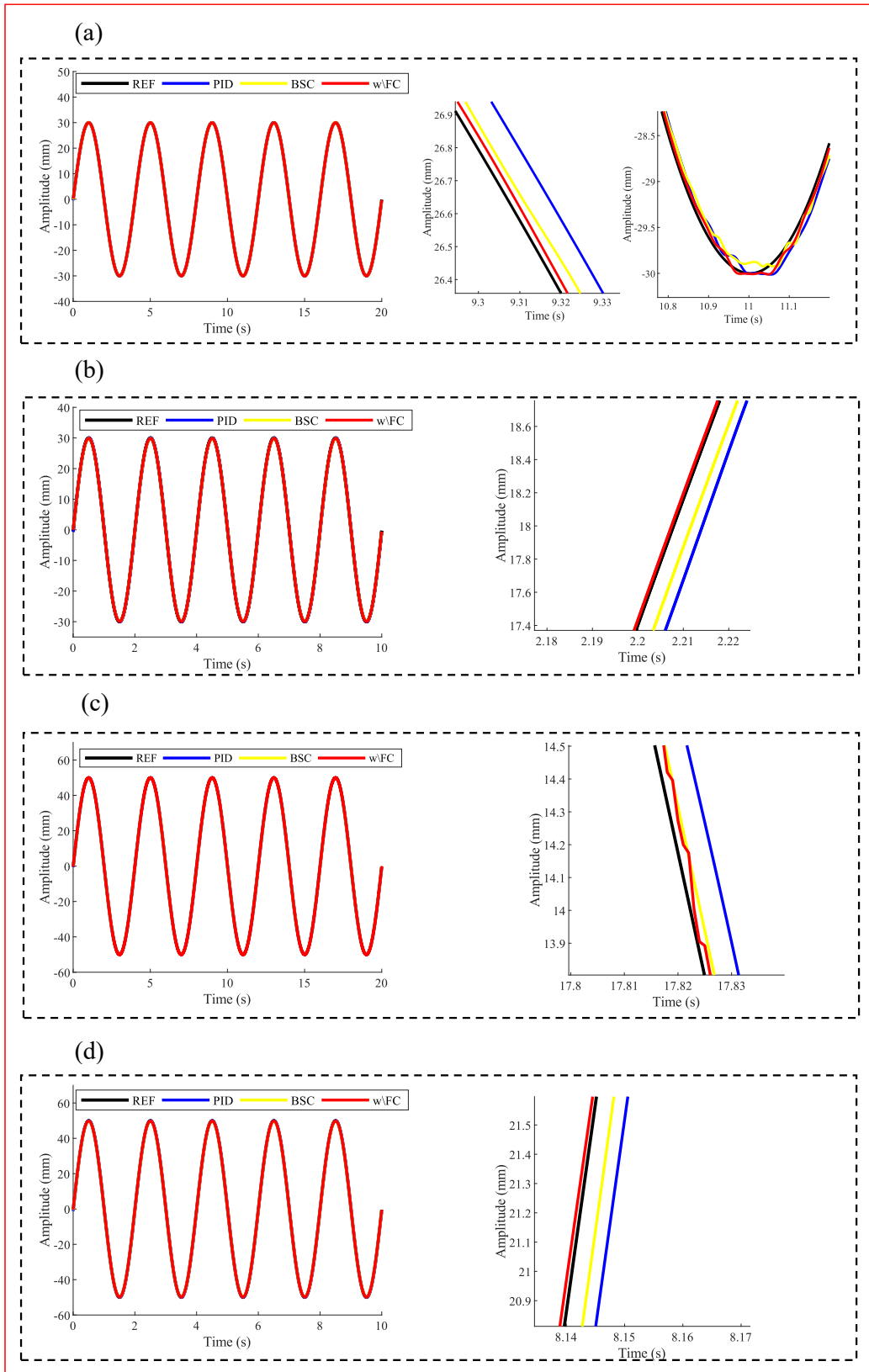
Figure 3. Position tracking (a) 30 mm and 0.25 Hz (b) 30 mm and 0.5 Hz (c) 50 mm and 0.25 Hz (d) 50 mm and 0.5 Hz.
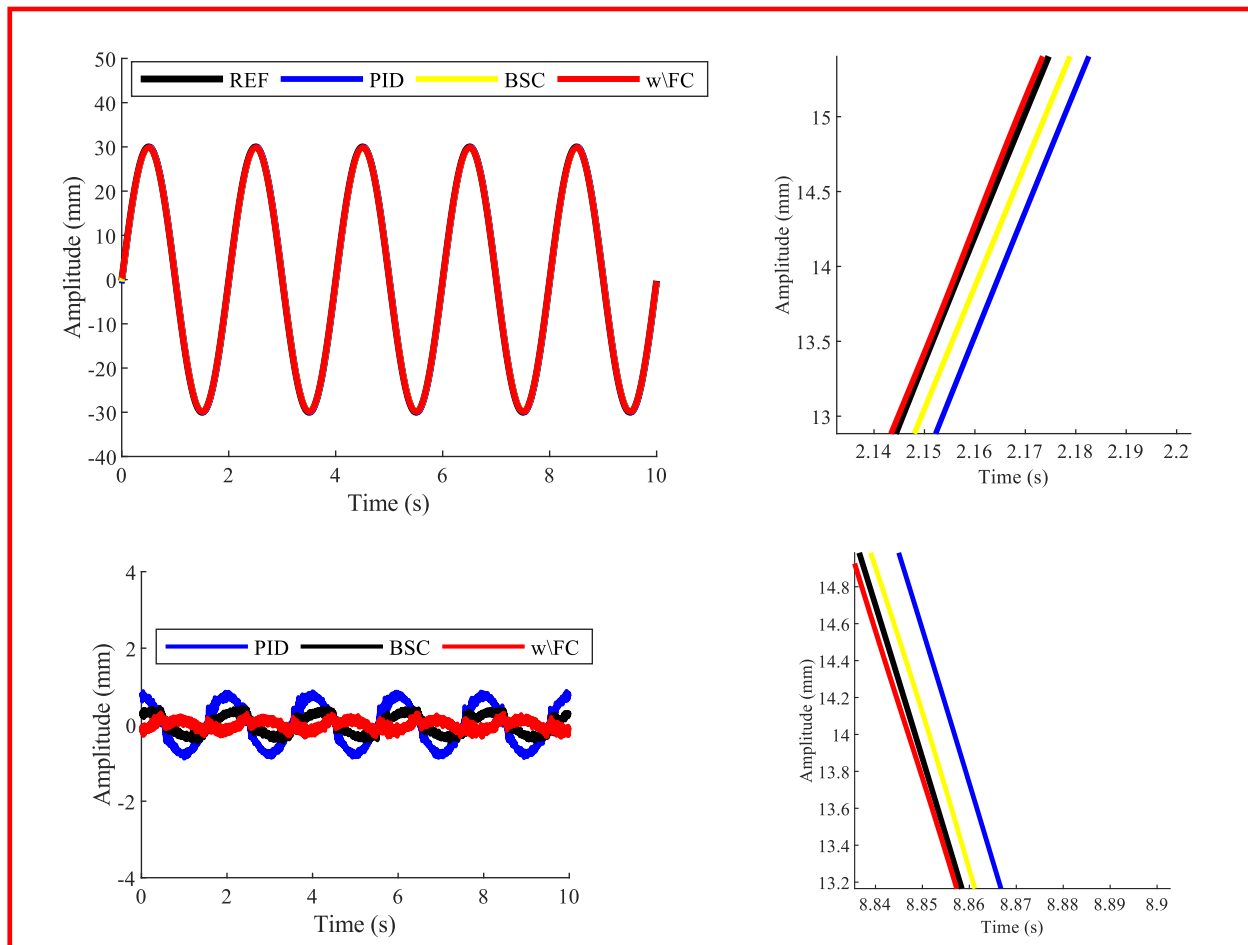
Figure 4. Position tracking and tracking error of 30 mm and 0.25 Hz with double load external disturbance.

5. DISCUSSION

This study improves electro-hydraulic position servo system precision control with an integral adaptive backstepping controller with friction compensation (w\FC). The PID controller offers the worst response due to its inability to handle system nonlinearities and friction. The w\FC controller outperforms both PID and traditional backstepping controllers due to its robustness, ability to handle nonlinearities, and friction compensation. It also has faster response time and the lowest performance measure index. Thus, for the tracking performance of the three controllers: the proposed integral adaptive backstepping controller with friction compensation > the traditional backstepping controller > the PID controller.

6. CONCLUSION

This paper presents a nonlinear integral adaptive backstepping controller designed to improve the position-tracking performance of EHSS. The controller uses a continuous approximation of the LuGre friction model, enhancing system performance. The design technique uses Lyapunov functions for stability and asymptotic tracking. Experimental results show the controller outperforms traditional backstepping controllers and conventional PID controllers under different working conditions.

Author Contributions
Michael Enyan: Methodology, Validation, Writing – original draft. **Luis Miguel Ruiz Páez:** Writing – review & editing, Formal analysis.

Declaration of Competing Interest
The authors declare that there are no competing financial interests.

Compliance with ethical standards
Research involving human participants and/or animals No human participants or animals were involved in this research.

REFERENCE

1. *Yao Z, Yao J, Yao F, Xu Q, Xu M, transactions W D-I and 2020 Model reference adaptive tracking control for hydraulic servo systems with nonlinear neural-networks ISA Transactions*

2. *Yao J, Jiao Z, Aeronautics S H-C J of and 2013 Friction compensation for low velocity control of hydraulic flight motion simulator: a simple adaptive robust approach Chinese Journal of Aeronautics*

3. *Truong H, Trinh H, Sciences K A-A and 2020 Safety operation of n-DOF serial hydraulic manipulator in constrained motion with consideration of contact-loss fault Applied Sciences*

4. *Sun C, Fang J, Wei J, Access B H-I and 2018 Nonlinear motion control of a hydraulic press based on an extended disturbance observer IEEE Access*

5. *Luo C, Yao J, Chen F, Li L, Access Q X-I and 2017 Adaptive repetitive control of hydraulic load simulator with RISE feedback IEEE Access*

6. *Chengwen W, Zongxia J, Long Q and Hongjun M 2018 Application of adaptive robust control for electro-hydraulic motion loading system Transactions of the Institute of Measurement and Control 40 873–84*

7. *Kang S, Yan H, Dong L, Processing C L-M S and S and 2018 Finite-time adaptive sliding mode force control for electro-hydraulic load simulator based on improved GMS friction model Mechanical Systems and Signal Processing*

8. *Sun W, Gao H, on O K-I transactions and 2014 Vibration isolation for active suspensions with performance constraints and actuator saturation IEEE/ASME Transactions on Mechatronics*

9. *Choi K, Oh J, Kim H-S, Han H-W, Park J-H, Lee G-H, Seo J and Park Y-J Experimental study on the dynamic characteristics of hydro-pneumatic semi-active suspensions for agricultural tractor cabins Applied Sciences*

10. *Ma X, Wong P, Processing J Z-M S and S and 2019 Practical multi-objective control for automotive semi-active suspension system with nonlinear hydraulic adjustable damper Mechanical Systems and Signal Processing Huang Y, Na J, Wu X, Industrial G G-I T on and 2018 Approximation-free control for vehicle active suspensions with hydraulic actuator IEEE Transactions on Industrial Electronics*

11. *Lovrec D, Modelling M K-I J of S and 2011 Modelling and simulating a controlled press-brake supply system International Journal of Simulation Modelling 10 133–44*

12. *Anon Merritt, H.E. (1967). Hydraulic Control Systems. Wiley, NewYork.*

13. *Feng H, Ma W, Yin C, Construction D C-A in and 2021 undefined Trajectory control of electro-hydraulic position servo system using improved PSO-PID controller Elsevier*

14. *Zahir A M, Alhady S, ... W O-I M & and 2018 Genetic algorithm optimization of PID controller for brushed DC motor Springer 0 427–37*

15. *Sungthong A, Science W A-P C and 2016 Particle swam optimization based optimal PID parameters for air heater temperature control system Procedia Computer Science*

16. *Truong D, Applications K A-E S with and 2011 Force control for press machines using an online smart tuning fuzzy PID based on a robust extended Kalman filter Expert Systems with Applications*

17. *Zhao J, Wang J, Mechatronics S W- and 2013 Fractional order control to the electro-hydraulic system in insulator fatigue test device Mechatronics*

18. *Das J, Santosh ·, Mishra K, Saha · R, Mookherjee · S and Sanyal · D 2017 Nonlinear modeling and PID control through experimental characterization for an electrohydraulic actuation system: System characterization with validation Journal of the Brazilian Society of Mechanical Sciences and Engineering 39 1177–87*

19. *Kaddissi C, Kenne J, on M S-I transactions and 2010 Indirect adaptive control of an electrohydraulic servo system based on nonlinear backstepping IEEE/ASME Transactions on Mechatronics*

20. *Wang N, Lin W, Institute J Y-J of the F and 2018 Sliding-mode-based robust controller design for one channel in thrust vector system with electromechanical actuators Journal of the Franklin Institute*

21. *Mohanty A, Mechanical B Y-A I and 2006 Integrated direct/indirect adaptive robust control (diarc) of hydraulic robotics arm with accurate parameter estimates Dynamic Systems and Control, Parts A and B*

22. *Yao J, Jiao Z, Ma D, on L Y-I T and 2013 High-accuracy tracking control of hydraulic rotary actuators with modeling uncertainties IEEE/ASME Transactions on Mechatronics*

23. *Lampaert V, ... J S-P of the 2004 and 2004 undefined Comparison of model and non-model based friction compensation techniques in the neighbourhood of pre-sliding friction ieeexplore.ieee.org*

24. *Wang J, Wang J, ... N D-I transactions on and 2004 Identification of pneumatic cylinder friction parameters using genetic algorithms IEEE/ASME Transactions on Mechatronics*

25. *Armstrong-Hélouvry B, Dupont P, Automatica C D W- and 1994 undefined A survey of models, analysis tools and compensation methods for the control of machines with friction Elsevier*

26. *Khayati K, Bigras P, on L D-I T and 2006 A multistage position/force control for constrained robotic systems with friction: Joint-space decomposition, linearization, and multiobjective observer/controller IEEE Transactions on Industrial Electronics*

27. *Dupont P and Dunlap E 1995 Friction modeling and PD compensation at very low velocities Journal of Dynamic Systems, Measurement, and Control*

28. *Zhang M, Zhou M, Liu H, Zhang B, Zhang Y and Chu H 2018 Friction compensation and observer-based adaptive sliding mode control of electromechanical actuator Advances in Mechanical Engineering 10 2018*

29. *Fei J, Ding H, Hou S, ... S W-I J of and 2012 Robust adaptive neural sliding mode approach for tracking control of a MEMS triaxial gyroscope International Journal of Advanced Robotic Systems*

30. *Karnopp D 1985 Computer simulation of stick-slip friction in mechanical dynamic systems*

31. *Bo L, Wear D P- and 1982 The friction-speed relation and its influence on the critical velocity of stick-slip motion Wear*

32. *Mostaghel N, structural T D-E engineering & and 1997 undefined Representations of Coulomb friction for dynamic analysis Wiley Online Library*

33. *Armstrong-Hélouvry B, Dupont P, Automatica C D W- and 1994 A survey of models, analysis tools and compensation methods for the control of machines with friction Automatica*

34. *Ferretti G, Magnani G, P R-I T 2004 Single and multistate integral friction models IEEE Transactions on Automatic Control*

35. *Li X, Yao J, Institute C Z-J of the F and 2017 undefined Output feedback adaptive robust control of hydraulic actuator with friction and model uncertainty compensation Elsevier*

36. *Dupont P, Hayward V, ... B A-I T 2002 Single state elastoplastic friction models IEEE Transactions on Automatic Control*

37. *Dahl P 1968 A solid friction model 158 3107–25*

38. *Wit C de, Olsson H, ... K A-I T 1995 A new model for control of systems with friction IEEE Transactions on Automatic Control*

39. *Wang X and Wang S 2012 High performance adaptive control of mechanical servo system with lugre friction model: Identification and compensation Journal of Dynamic Systems, Measurement and Control, Transactions of the ASME 134*

40. *Yao J, Jiao Z and Han S 2013 Friction compensation for low velocity control of hydraulic flight motion simulator: A simple adaptive robust approach Chinese Journal of Aeronautics 26 814–22*

41. *Khayati K, Bigras P and Dessaint L A 2009 LuGre model-based friction compensation and positioning control for a pneumatic actuator using multi-objective output-feedback control via LMI optimization Mechatronics 19 535–47*

42. *Schindele D and Aschemann H 2009 Adaptive friction compensation based on the LuGre model for a pneumatic rodless cylinder IECON Proceedings (Industrial Electronics Conference) 1432–7*

43. *Yang G 2020 Dual extended state observer-based backstepping control of electro-hydraulic servo systems with time-varying output constraints Transactions of the Institute of Measurement and Control 42 1070–80*

44. *Merritt H E 1967 "Hydraulic Control Systems,". John Wiley & Sons*

45. *Yao B, Bu F, Reedy J Adaptive robust motion control of single-rod hydraulic actuators: theory and experiments IEEE/ASME Transactions on Mechatronics 5 79*

46. *Yang G 2020 Dual extended state observer-based backstepping control of electro-hydraulic servo systems with time-varying output constraints Transactions of the Institute of Measurement and Control 42 1070–80*

47. *Yao J, Jiao Z and Han S 2013 Friction compensation for low velocity control of hydraulic flight motion simulator: A simple adaptive robust approach Chinese Journal of Aeronautics 26 814–22*